



Contents lists available at ScienceDirect



Comparison studies of adsorption properties of MgO nanoparticles and ZnO–MgO nanocomposites for linezolid antibiotic removal from aqueous solution using response surface methodology

Ali Fakhri^{a,b,*}, Sajjad Behrouz^c^a Department of Chemistry, Shahr-e-Qods Branch, Islamic Azad University, Tehran, Iran^b Young Researchers and Elite Club, Science and Research Branch, Islamic Azad University, Tehran, Iran^c Department of Biology, Central Tehran Branch, Islamic Azad University, Tehran, Iran

ARTICLE INFO

Article history:

Received 18 July 2014

Received in revised form 16

November 2014

Accepted 12 December 2014

Available online 19 December 2014

Keywords:

Box–Behnken Design

Response surface methodology

Aqueous solution

Adsorption

Antibiotic

MgO nanoparticles

Kinetics studies

ABSTRACT

In this investigation, the adsorption measure of linezolid antibiotic onto MgO nanoparticles and ZnO–MgO nanocomposites were performed. The adsorbents were characterized by different techniques such as XRD, SEM, TEM and BET. The parameters influence such as the pH, adsorbent dosage and temperature was tested and evaluated by Box–Behnken Design combined with response surface methodology. Performing adsorption tests at optimal conditions set as 0.5 g L⁻¹ of adsorbent, pH 10 and 308 K make admit to obtain high adsorption turnover (123.45 and 140.28 mg g⁻¹ for MgO nanoparticles and ZnO–MgO nanocomposites, respectively). A good compromise between predicted and experimental data in this research was observed. The experimental equilibrium data fitting to Langmuir, Freundlich, Tempkin and Dubinin–Radushkevich models indicate that the Langmuir model is a best model for evaluation of adsorption behavior. Kinetic evaluation of experimental data indicated that the adsorption operations followed well pseudo-second-order models. The adsorption capacity of ZnO–MgO nanocomposites is higher than MgO nanoparticles that because of the ZnO–MgO nanocomposites have high specific surface area.

© 2014 The Institution of Chemical Engineers. Published by Elsevier B.V. All rights reserved.

1. Introduction

Newly, the capable association has become enhancing fond about the possible general health strike of novel environmental pollutants emanated from artful, human activities and agricultural. (Jones et al., 2005; Khetan and Collins, 2007; Zylan and Ince, 2011). Numerous pharmaceuticals were found ubiquitously up to μg L⁻¹ level in aqueous environment (Halling-Sorensen et al., 1998; Ternes, 1998; Kolpin et al., 2002; Fent et al., 2006; Nikolaou et al., 2007; Carabineiro et al., 2011, 2012), in soil (Halling-Sorensen et al., 1998; Thiele-Bruhn, 2003) and as high as 100 μg L⁻¹ in effluent from drug manufactures (Larsson et al., 2007). Linezolid is used to treat infections, including pneumonia,

and infections of the skin and blood. Linezolid is in a class of antibiotics called oxazolidinones (Table 1). The removal of linezolid is important that because of this antibiotic is dangerous drug interaction could occur, leading to serious side effects.

The methods of controlling water pollution fall into three general categories: physical, chemical, and biological. Chemical reactions can be used to remove pollutants from water. The results of chemical reactions were high efficiency. In order that to assess the experiment parameters effect on adsorption turnover, the appropriate apply of a proportionate experimental design is of particular importance. Response Surface Methodology (RSM), a statistical techniques and collection of mathematical, has been found to be an effective method

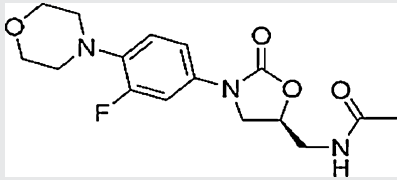
* Corresponding author at: Department of Chemistry, Shahr-e-Qods Branch, Islamic Azad University, Tehran, Iran. Tel.: +98 21 22873079; fax: +98 21 22873079.

E-mail address: ali.fakhri88@yahoo.com (A. Fakhri).

<http://dx.doi.org/10.1016/j.psep.2014.12.007>

0957-5820/© 2014 The Institution of Chemical Engineers. Published by Elsevier B.V. All rights reserved.

Table 1 – Physicochemical properties of linezolid.

	Molecular weight (g mol ⁻¹)	Density (g/cm ³)	Chemical structure
Linezolid	337.346	1.302	

for studying the mutual interaction between the parameter and optimizing the variables in the adsorption process. The MgO nanoparticles and ZnO–MgO nanocomposites have the inexpensive and easy synthesis. Then, these nano powders were considered for removal of antibiotics. This contribution was aimed at the investigation of linezolid antibiotic adsorption performances over MgO nanoparticles and ZnO–MgO nanocomposites. The Box–Behnken Design (BBD) of the RSM was employed to investigate the effects of important operating parameters including pH, adsorbent dose, and temperature on linezolid adsorption capability.

2. Materials and methods

2.1. Native materials

Analytical reagent grade of magnesium chloride anhydrous, zinc acetate dehydrate, ammonia, and polyvinyl pyrrolidone (PVP) were obtained from Merck. Linezolid (99%) were obtained from Leap Labchem Co., Ltd., and used as received. Water used in the study was purified by distillation.

2.2. Purveyance of MgO nanoparticles

200 mL solution of MgCl₂ (1 M) was derived in 1 L flat bottomed flask and 200 mg of PVP was added within it. The poly vinyl pyrrolidone has used as inhibitor for the growth the crystallites of magnesium hydroxide during the course of sedimentation. The mixture was stirred for 30 min, and NaOH is added by dropwise. The white precipitate was washing using double distilled water, and during 24 h dried an oven with 70 °C and eventually calcined at 500 °C for 2 h to get MgO nanoparticles.

2.3. Purveyance of ZnO–MgO nanocomposites

First, a 100 mL aliquot containing zinc acetate solution and amount of MgO nanoparticles and PVP were mixture for 30 min. Then, nano-sized Zn(OH)₂ was formed. At the end, the mixture was during 24 h dried an oven with 70 °C. The obtained precipitate was calcined at 550 °C for 4 h. A scanning electron microscope (SEM); JEOL JSM-5600 Japan Digital Scanning Electron Microscope, X-ray diffractometer (XRD) Philips X'Pert, USA and transmission electron microscopy (TEM, JEM-2100F HR, 200 KV) were used to characterize the nano powders for its morphological information. Brunauer–Emmett–Teller (BET) surface area (S_{BET}) of the powder was analyzed by nitrogen adsorption in an ASAP2020 surface area and porosity analyzer (Micromeritics, USA).

2.4. Equilibrium studies

The antibiotic removal using MgO nanoparticles and ZnO–MgO nanocomposites was survey by batch methods.

Various concentrations (10, 30, 50 and 100 mg L⁻¹) of antibiotics solutions were prepared. The dosage of adsorbent in between 0.2 to 0.8 g L⁻¹ was added with pH variable in between 3 and 10. The amount of adsorbate removal was computed using the Eq. (1) (Fakhri and Adami, 2014):

$$q_e = \frac{(C_0 - C_e)}{w} \quad (1)$$

where *w* is the mass of the adsorbent (g), *v* is the volume of solution (L) and *C*₀ and *C*_e are the adsorbate concentrations in mg L⁻¹ initially and at a given time. The analysis of data was performed by analysis of relevance employing least-square model and the standard deviation of Marquardt's percent is computed by the Eq. (2) (Mall et al., 2005):

$$\text{MPSD} = 100 \sqrt{\frac{1}{n-p} \sum_{i=1}^n \left(\frac{q_{e,\text{exp}} - q_{e,\text{cal}}}{q_{e,\text{exp}}} \right)_i^2} \quad (2)$$

This error function is analogous in some tribute to a geometric average fallacy dispensation reclaimed pursuant to the degrees number of system freedom.

2.5. Box–Behnken Design and linezolid antibiotic adsorption optimization

RSM was employed to investigate the effects of different operating factors on linezolid adsorption turnover, and disclose the optimum conditions for linezolid removal. BBD was used to evaluate the major effects of adsorption variables and optimize the adsorption reaction. The effects of variables (adsorbent dose, pH value and temperature) on adsorption turnover were selected for RSM. The range and levels for these variables are coded according to Eq. (3) and summarized in Table 2.

$$X_i = \frac{X_i - X_0}{\Delta X} \quad (3)$$

where *X*_i are the coded and the real values of variables. *X*₀ are the center point of *X*_i and the step change in *X*_i respectively. The relationship between the response Y (linezolid adsorption amount) and these variables parameters can be distinguished

Table 2 – Process variables and their level for the linezolid adsorption by BBD.

Factor	Low level (-1)	Medium level (0)	High level (+1)
Temperature (A)	288 K	298 K	308 K
Adsorbent dose (B)	0.2 g L ⁻¹	0.5 g L ⁻¹	0.8 g L ⁻¹
pH (C)	3	6.5	10

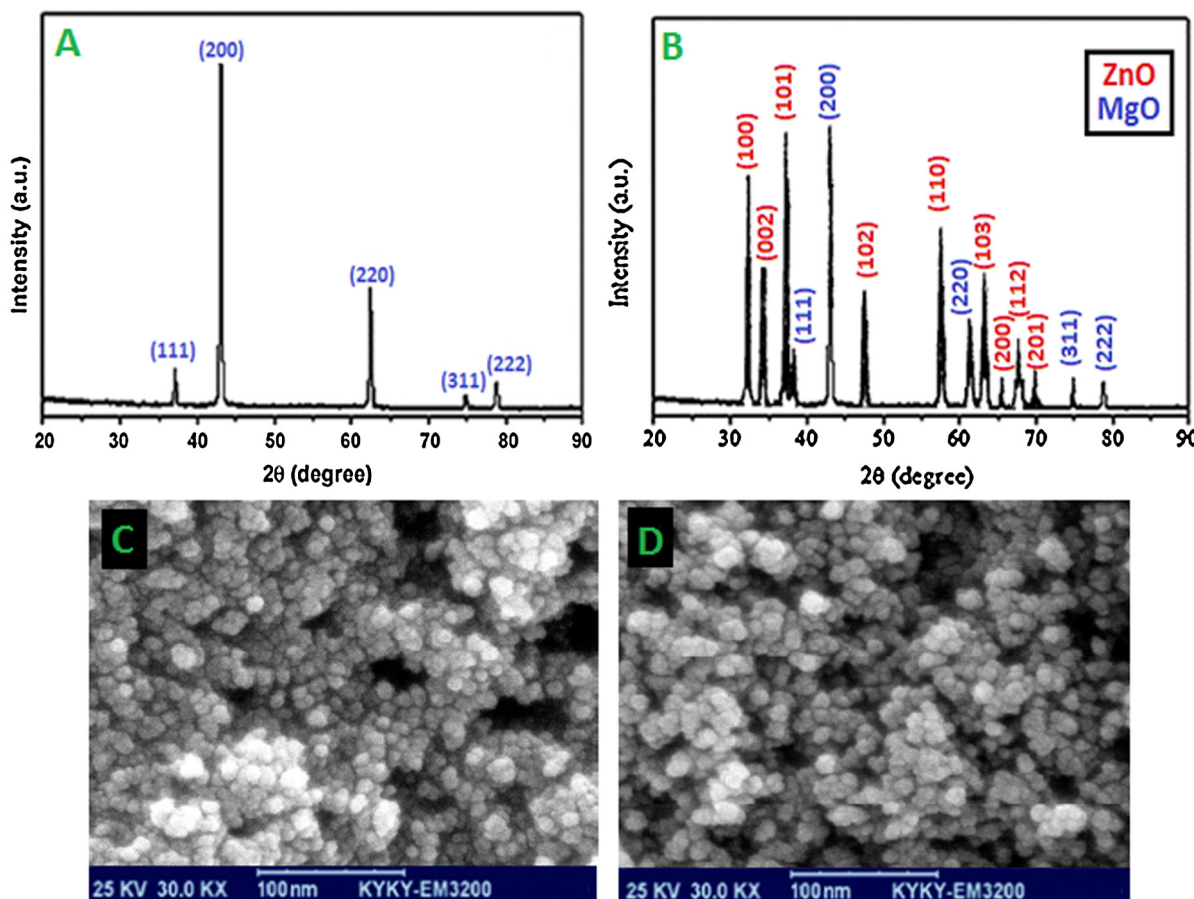


Fig. 1 – XRD pattern of MgO nanoparticles (A), ZnO–MgO nanocomposites (B) and SEM images of MgO nanoparticles (C), ZnO–MgO nanocomposites (D).

by the following second-order polynomial equation:

$$Y = \beta_0 + \beta_1 A + \beta_2 B + \beta_3 C + \beta_{11} A^2 + \beta_{22} B^2 + \beta_{33} C^2 + \beta_{12} AB \\ + \beta_{13} AC + \beta_{23} BC \quad (4)$$

The validity of this equation was tested by using ANOVA (analysis-of-variance), and fit quality of the equation was judged from the coefficients of correlation and p-value.

3. Results and discussion

3.1. Characterizations of MgO nanoparticles and ZnO–MgO nanocomposites

The X-ray diffraction (XRD) patterns for MgO nanoparticles are indicated in Fig. 1A. The XRD peaks are labeled to (111), (200), (220), (311) and (222) reflections [JCPDS Card No. 4-0829]. XRD patterns of the ZnO/MgO nanocomposite is shown in Fig. 1B which demonstrates the presence of wurtzite ZnO peaks and cubic MgO peaks. The ZnO and MgO phases were with clarity determined by the presence of wurtzite ZnO (101), (100), (002) [JCPDS Card No. 36-1451] and MgO peaks. The crystallite sizes of MgO and ZnO/MgO specimens have been distinguished using the Scherrer's equation: $D = 0.9\lambda/B \cos \theta$; where D is the crystallite size (nm), λ is the wavelength of the X-ray radiation, θ is the Bragg's angle and B is the full width at half maximum (FWHM) of the peak at 2θ . The crystallite sizes of MgO and ZnO/MgO have been estimated as 29 and 30 nm, respectively. The SEM micrographs for the prepared samples are shown in Fig. 1C and D. The particles are agglomerated

into bundles of flaky-spherical morphology. The particle size of the MgO sample was typically in the between of 25–30 nm. As can see, it was found that the harsh morphology and the rough particle sizes were not changed with doping ZnO.

Fig. 2(A) and (B) show typical TEM images of MgO nanoparticles and ZnO–MgO nanocomposites, respectively. The images indicated spheroidal morphologies. The crystallite sizes of samples particles were found to be ranging from 25 to 30 nm. Fig. 2(C) demonstrates the nitrogen sorption isotherms and the related to pore size distributions of the obtained MgO nanoparticles and ZnO–MgO nanocomposites samples. The isotherms of samples exhibit type III characteristics with a significant type H3 loop. The specific surface area and total pore volume of MgO nanoparticles and ZnO–MgO nanocomposites computed using the multipoint BET-equation is 48 and $153 \text{ m}^2 \text{ g}^{-1}$ and 0.30 and $0.65 \text{ cm}^3 \text{ g}^{-1}$, respectively.

3.2. Regression model

The major objective of RSM is to distinguish regression model of adsorption reaction, and the quadratic model was applied to find out the relationship between the response and variables. Pursuant to experiment data, the final empirical model of linezolid adsorption over MgO nanoparticles and ZnO–MgO nanocomposites was described by using Eq. (5) and (6).

$$Y = +54.12600 + 1.49375A - 0.23000B + 1.47875C + 0.26250AB \\ - 0.19500AC + 0.082500BC + 1.72700A^2 - 2.84550B^2 \\ + 1.85200C^2 \quad (5)$$

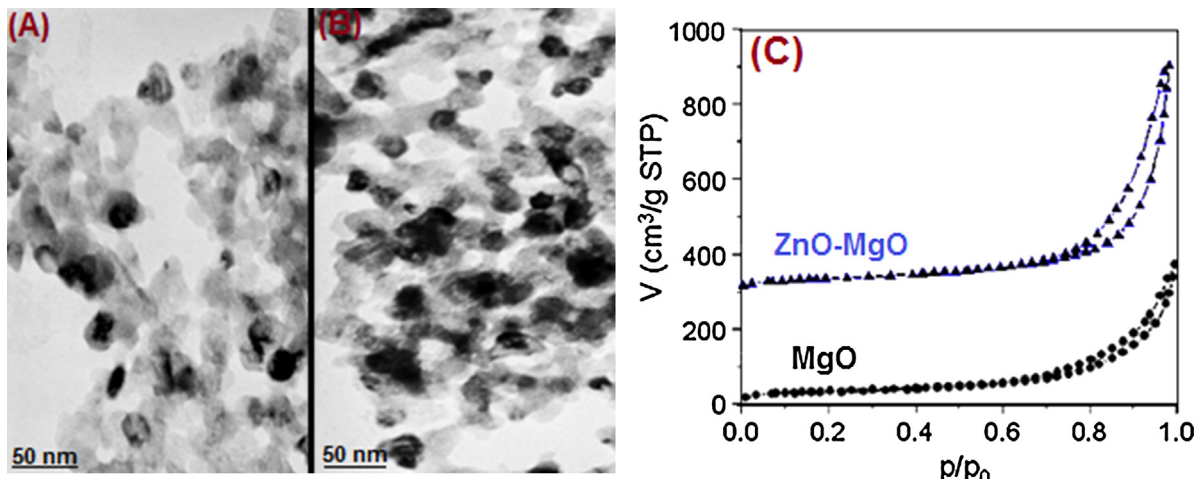


Fig. 2 – TEM images of MgO nanoparticles (A), ZnO–MgO nanocomposites (B) and nitrogen sorption isotherms of two samples (C).

$$\begin{aligned} Y = & +57.12600 + 1.49375A - 0.23000B + 1.47875C + 0.26250AB \\ & - 0.19500AC + 0.082500BC + 1.72700A^2 - 2.84550B^2 \\ & + 1.85200C^2 \end{aligned} \quad (6)$$

where, Y is the predicted response (linezolid adsorption capacity). In order to ensure the efficiency of employed model, an adequate fit of the model should be given to avoid poor or ambiguous results. The Eqs. (5) and (6) are very important and were determined by using BBD in Response Surface Methodology (RSM) by Design Expert Version 6.0.10 (Stat Ease, USA). The importance of quadratic regression model was analyzed by the value of F , p and correlation coefficient, and the corresponding results of ANOVA were tabulated in Table 3. The model F -value (24.30) and a very low p -value (less than 0.0001) implicit that the model was highly significant for linezolid adsorption on MgO nanoparticles and ZnO–MgO nanocomposites. The value of determination coefficient ($R^2 = 0.9690$) of Eqs. (5) and (6) indicates that the regression model is best suited for predicting the performance of linezolid adsorption on MgO nanoparticles and ZnO–MgO nanocomposites. As can be seen from Table 3, all the p -values of A , C , A^2 , B^2 , and C^2 are less than 0.05, which indicates that these variables are significant and have great influence on linezolid adsorption capacity. The good agreement and high correlation coefficient of plot of experimental values versus predicted removal amount suggest high efficiency of above mention equation to evaluate and explain experimental data (Fig. 3).

3.3. Response surface methodology

The inflection natures of Fig. 4 indicate the RSM plots of adsorption capacity versus significant variables confirm strong interaction between the variables. The composed influence of adsorbent dosage and temperature on the linezolid uptake by the nanoparticles is shown in Fig. 4(A and B). It may be noted that the removal of the linezolid reduced with increase in temperature as earlier. In a solution of constant linezolid concentration, an enhancing in removal amount with increase in adsorbent dosage might be due to accessibility of rather active site at higher mass of adsorbent. The response surface plots (Fig. 4C and D, changes in the amount of removal as a function of adsorbent dosage) indicate that removal turnover has positive

correlation with dose of adsorbent, so that adsorption enhanced with increasing adsorbent dosage. At higher value maybe due to enhance in surface area and availability of more active adsorption sites. Fig. 4(E and F) shows the interaction of pH with temperature and their relation with adsorption turnover. The pH has positive correlation with adsorption turnover and at higher pH and high

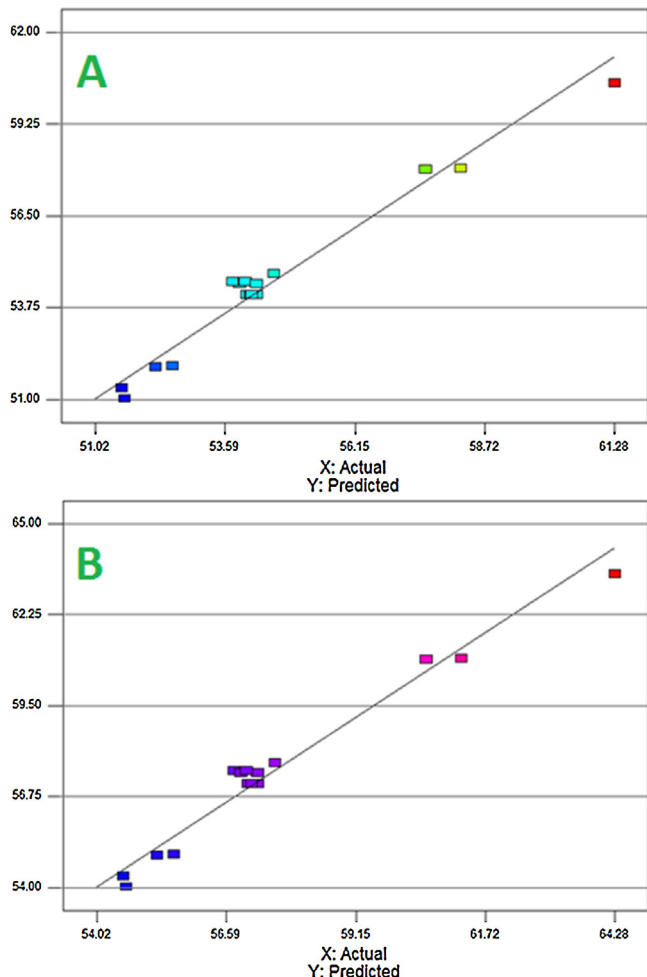


Fig. 3 – The predicted values versus experimental values of linezolid adsorption on MgO nanoparticles (A) and ZnO–MgO nanocomposites (B).

Table 3 – The results of ANOVA for the response surface quadratic model.

Source	Sum of squares	DF ^a	Mean square	F value ^b	p-value Prob > F ^c
Model	94.39	9	10.49	24.30	0.0002
A	17.85	1	17.85	41.36	0.0004 ^s
B	0.42	1	0.42	0.98	0.3551
C	17.49	1	17.49	40.53	0.0004 ^s
AB	0.28	1	0.28	0.64	0.4505
AC	0.15	1	0.15	0.35	0.5714
BC	0.027	1	0.027	0.063	0.8089
A^2	12.56	1	12.56	29.10	0.0010 ^s
B^2	34.09	1	34.09	78.99	<0.0001 ^s
C^2	14.44	1	14.44	33.46	0.0007 ^s
Residual	3.02	7	0.43		
Lack of fit	3.00	3	1.00	164.31	0.0001
Pure error	0.024	4	6.080E–003		
Corr. total	97.41	16			

^a Degree of freedom.^b Test for comparing model with residual (error) variance.^c Probability of finding the observed F value when the null hypothesis is true.^s Significant at $p < 0.05$.

temperature led to achievement of higher adsorption turnover. High removal amount of linezolid at high pH shows that the surface in alkaline medium causing reduce the protonation at their surfaces due to neutralization of positive charges, resulting in easier diffusion.

3.4. Adsorption equilibrium study

Adsorption parameters attained by well-known equation of traditionally known isotherms give useful information about mechanism and properties and tendency of adsorbent. Based on the linear form of Langmuir isotherm model (according to Table 4), the values of K_L (the Langmuir adsorption constant (L mg^{-1})) and q_m (theoretical maximum monolayer adsorption capacity (mg g^{-1})) were obtained from the intercept and slope of the plot of C_e/q_e versus C_e , respectively (Fakhri, 2013). The high correlation coefficients (R^2) (0.9985 and 0.9990 for MgO nanoparticles and ZnO–MgO nanocomposites, respectively) show the applicability of Langmuir model for interpretation of the experimental data. The parameters of Freundlich isotherm model such as K_F ($(\text{mg g}^{-1})/(\text{mg L}^{-1})^{1/n}$) and n (the capacity and intensity of the adsorption) were calculated from the intercept and slope of the linear plot of $\ln q_e$ versus $\ln C_e$, respectively and their values are presented in Table 4. The value of $1/n$ for Freundlich isotherm (Freundlich, 1906) confirm

the high tendency of linezolid for transfer to the adsorbents surface, while lower R^2 value indicates its unsuitability for fitting the experimental data. The heat of the adsorption and the adsorbent–adsorbate interaction were evaluated by using Tempkin isotherm model (Fakhri, 2014). In this model B is the Tempkin constant related to heat of the adsorption (J mol^{-1}), T is the absolute temperature (K), R is the universal gas constant ($8.314 \text{ J mol}^{-1} \text{ K}^{-1}$), K_T is the equilibrium binding constant (L mg^{-1}). The values of the Tempkin constants and the correlation coefficient are lower than the Langmuir value. Then, the Tempkin isotherm has poor ability. Another adsorption isotherm as D–R (Dubinin and Radushkevich, 1974; Sari and Tuzen, 2014) model was used to estimate the porosity apparent free energy and the characteristic of adsorption. In the D–R isotherm K ($\text{mol}^2 (\text{kJ})^{-1}$) is a constant related to the adsorption energy, Q_s (mg g^{-1}) is the theoretical saturation capacity, e is the Polanyi potential. The slope of the plot of $\ln q_e$ versus e^2 gives K and the intercept yields the Q_s value. The lower value of R^2 of D–R model indicate not usefulness of this model to fit the experimental data.

3.5. Adsorption kinetic modeling

Kinetic evaluated based on two models (pseudo first and second-order) give good and deep knowledge about the

Table 4 – Isotherm constant parameters and R^2 calculated for the adsorption of linezolid.

Isotherms	Equations	Parameters	MgO nanoparticles	ZnO–MgO nanocomposites
Langmuir	$C_e/q_e = 1/(q_m) + C_e/q_m$	$q_m (\text{mg g}^{-1})$	123.45	140.28
		$K_L (\text{L mg}^{-1})$	0.1663	0.2052
		R^2	0.9985	0.9990
Freundlich	$\ln q_e = \ln K_F + (1/n) \ln C_e$	$1/n$	0.695	0.702
		$K_F (\text{L mg}^{-1})$	15.839	16.022
		R^2	0.9783	0.9755
Tempkin	$q_e = B_1 \ln K_T + B_1 \ln C_e$	B_1	2.589	2.855
		$K_T (\text{L mg}^{-1})$	919.51	990.27
		R^2	0.9588	0.9508
Dubinin and Radushkevich (D–R)	$\ln q_e = \ln Q_s - B e^2$	$Q_s (\text{mg g}^{-1})B (\text{mol}^2 (\text{kJ})^{-1})$	89.56	95.87
		R^2	5E–9	6E–3
			0.9055	0.9171

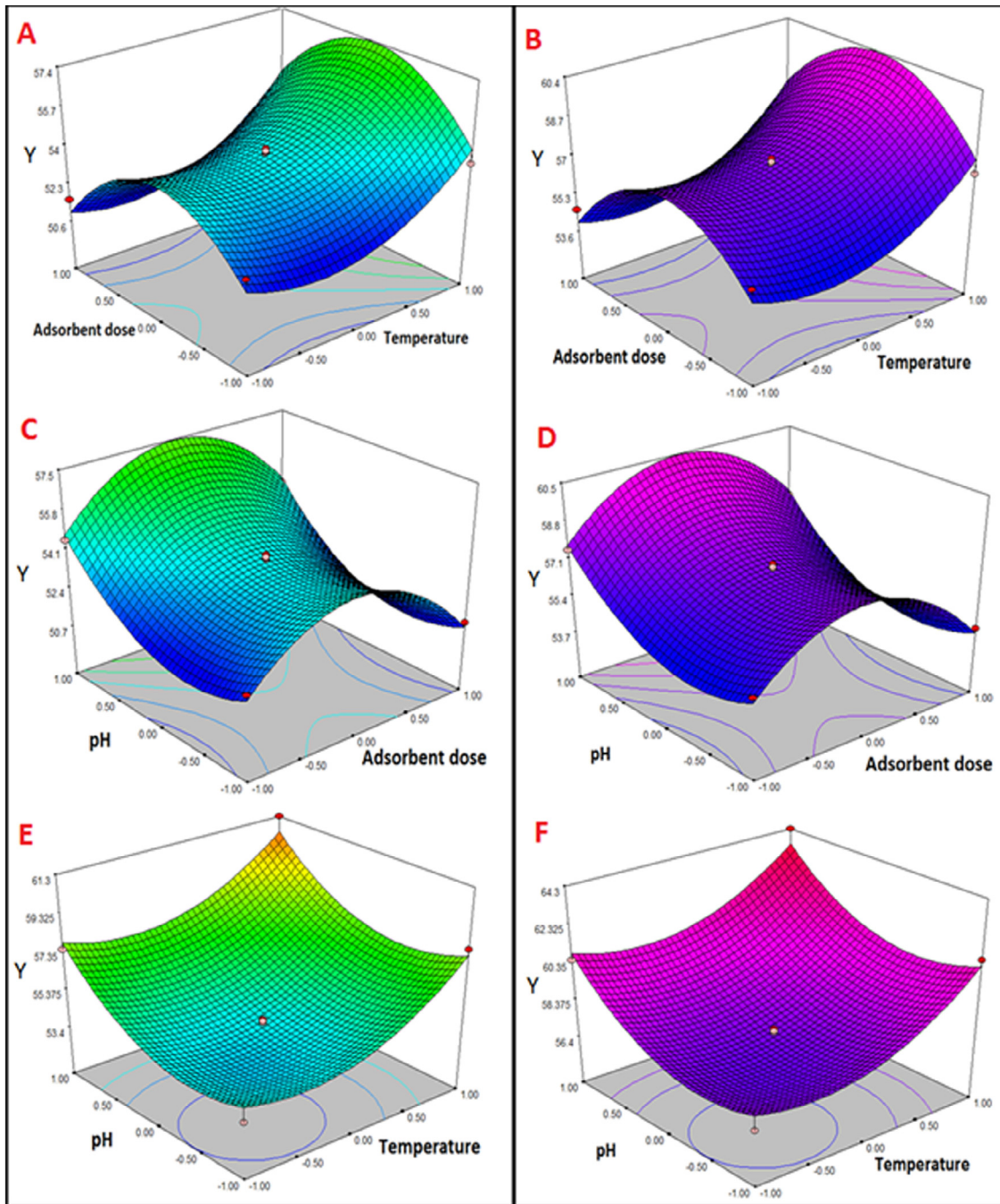


Fig. 4 – Response surface plots for the adsorption of linezolid using MgO nanoparticles (right) and ZnO–MgO nanocomposites (left): adsorbent dose–temperature (A and B); pH–adsorbent dose (C and D); pH–temperature (E and F).

Table 5 – Kinetic parameters for the adsorption of linezolid onto MgO nanoparticles ($q_{\text{exp}} = 31.58 \text{ mg g}^{-1}$) and ZnO–MgO nanocomposites ($q_{\text{exp}} = 33.91 \text{ mg g}^{-1}$).

Kinetics model	Equations	Parameters	MgO nanoparticles	ZnO–MgO nanocomposites
Pseudo-first-order	$\ln(q_e - q_t) = \ln(q_e) - k_1 t$	q_e (calc)	24.52	26.85
		k_1	0.0909	0.1112
		R^2	0.9886	0.9893
		MPSD	18.54	19.23
Pseudo-second-order	$(t/q_t) = 1/(k_2 q_e^2) + 1/q_e(t)$	q_e (calc)	33.22	36.02
		k_2	0.0006	0.0009
		R^2	0.9973	0.9981
		MPSD	1.851	1.951

rate and mechanism of an adsorption process. Table 5 summarized the properties of each model. In the pseudo-first-order model (Lagergren model), by plotting the values of $\log(q_e - q_t)$ versus t may give a linear relationship that its slope and intercept is used to evaluate the k_1 and q_e values (Table 5) (Sari and Tuzen, 2013). The interval among experimental q_e value with intercept show that this model not suitable to explain experimental data. The enhance in the value of k_1 and k_2 attributed to increase in driving force of mass transfer. The sorption kinetics may be described by a pseudo second-order model (Sari and Tuzen, 2013). In despite of first order model, the plot of t/q_t versus t for the pseudo-second-order kinetic model gives a straight line with a high correlation coefficient that k_2 and equilibrium adsorption capacity (q_e) were computed from the intercept and slope of this line, respectively (Sari and Tuzen, 2013). The values of R^2 and closeness of experimental and theoretical adsorption capacity (q_e) value indicate the applicability of the pseudo-second-order model to explain (Table 5).

4. Conclusion

The combination of various effects in addition to application of MgO nanoparticles and ZnO–MgO nanocomposites are fast, sensitive and efficient adsorption method for the linezolid removal. The effects of experimental parameters on the removal amount were performed using BBD combined with RSM. The optimum operating variables to obtain maximum linezolid removal were distinguished. The equilibrium data were best described by the Langmuir model, while the appropriate kinetic model for fitting the experimental data is pseudo-second order model. The benefit of method is possibility to use nontoxic adsorbent for removal of large amount of linezolid in short time via a simple procedure.

Acknowledgment

Authors thank the Islamic Azad University Shahr-e-Qods Branch for providing facility to carry out our research.

References

- Carabineiro, S.A.C., Thavorn-Amornsri, T., Pereira, M.F.R., Figueiredo, J.L., 2011. Adsorption of ciprofloxacin on surface-modified carbon materials. *Water Res.* 45, 4583–4591.
- Carabineiro, S.A.C., Thavorn-amornsri, T., Pereira, M.F.R., Serp, P., Figueiredo, J.L., 2012. Comparison between activated carbon, carbon xerogel and carbon nanotubes for the adsorption of the antibiotic ciprofloxacin. *Catal. Today* 186, 29–34.
- Dubinin, M.M., Radushkevich, L.V., 1974. The equation of the characteristic curve of the activated charcoal. *Proc. USSR Phys. Chem. Sect.* 55, 331–337.
- Fakhri, A., Adami, S., 2014. Adsorption and thermodynamic study of Cephalosporins antibiotics from aqueous solution onto MgO nanoparticles. *J. Taiwan Inst. Chem. Eng.* 45, 1001–1006.
- Fakhri, A., 2013. Adsorption characteristics of graphene oxide as a solid adsorbent for aniline removal from aqueous solutions: kinetics, thermodynamics and mechanism studies. *J. Saudi Chem. Soc.*, <http://dx.doi.org/10.1016/j.jscs.2013.10.002>.
- Fakhri, A., 2014. Application of response surface methodology to optimize the process variables for fluoride ion removal using maghemite nanoparticles. *J. Saudi Chem. Soc.* 18, 340–347.
- Fent, K., Weston, A.A., Caminada, D., 2006. Ecotoxicology of human pharmaceuticals. *Aquat. Toxicol.* 76, 122–159.
- Freundlich, H., 1906. Über die adsorption in lösungen (adsorption in solution). *Z. Phys. Chem.* 57, 384–470.
- Halling-Sørensen, B., Nors Nielsen, S., Lanzky, P.F., Ingerslev, F., Holten Lutzhoff, H.C., Jorgensen, S.E., 1998. Occurrence, fate and effects of pharmaceutical substances in the environment—a review. *Chemosphere* 36, 357–393.
- Jones, O.A.H., Voulvoulis, N., Lester, J.N., 2005. Human pharmaceuticals in wastewater treatment processes. *Crit. Rev. Environ. Sci. Technol.* 35, 401–427.
- Khetan, S.K., Collins, T.J., 2007. Human pharmaceuticals in the aquatic environment: a challenge to green chemistry. *Chem. Rev.* 107, 2319–2364.
- Kolpin, D.W., Furlong, E.T., Meyer, M.T., Thurman, E.M., Zaugg, S.D., Barber, L.B., Buxton, H.T., 2002. Pharmaceuticals, hormones, and other organic wastewater contaminants in U.S. streams, 1999–2000: a national reconnaissance. *Environ. Sci. Technol.* 36, 1202–1211.
- Larsson, D.G.J., de Pedro, C., Paxeus, N., 2007. Effluent from drug manufactures contains extremely high levels of pharmaceuticals. *J. Hazard. Mater.* 148, 751–755.
- Mall, I.D., Srivastava, V.C., Agarwal, N.K., Mishra, I.M., 2005. Adsorptive removal of malachite green dye from aqueous solution by bagasse fly ash and activated carbon-kinetic study and equilibrium isotherm analyses. *Colloids Surf. A: Physicochem. Eng. Asp.* 264, 17–28.
- Nikolaou, A., Meric, S., Fatta, D., 2007. Occurrence patterns of pharmaceuticals in water and wastewater environments. *Anal. Bioanal. Chem.* 387, 1225–1234.
- Sari, A., Tuzen, M., 2013. Adsorption of silver from aqueous solution onto raw vermiculite and manganese oxide-modified vermiculite. *Microporous Mesoporous Mater.* 170, 155–163.
- Sari, A., Tuzen, M., 2014. Cd(II) adsorption from aqueous solution by raw and modified kaolinite. *Appl. Clay Sci.* 89, 63–72.
- Ternes, T.A., 1998. Occurrence of drugs in German sewage treatment plants and rivers. *Water Res.* 32, 3245–3260.
- Thiele-Bruhn, S., 2003. Pharmaceutical antibioticcompounds in soils – a review. *J. Plant Nutr. Soil Sci.* 166, 145–167.
- Ziyylan, A., Ince, N.H., 2011. The occurrence and fate of anti-inflammatory and analgesic pharmaceuticals in sewage and fresh water: treatability by conventional and nonconventional processes. *J. Hazard Mater.* 187, 24–36.